BIOMATERIALS SYNTHESIS AND CHARACTERIZATION

Osseointegration of titanium implants functionalised with phosphoserine-tethered poly(epsilon-lysine) dendrons: a comparative study with traditional surface treatments in sheep

Stefan Stübinger · Katja Nuss · Alexander Bürki ·
Isabel Mosch · Miché le Sidler · Steve T. Meikle ·
Brigitte von Rechenberg · Matteo Santin

Abstract The aim of this study was to analyse the osseo-integrative potential of phosphoserine-tethered dendrons when applied as surface functionalisation molecules on titanium implants in a sheep model after 2 and 8 weeks of implantation. Uncoated and dendron-coated implants were implanted in six sheep. Sandblasted and etched (SE) or porous additive manufactured (AM) implants with and without additional dendron functionalisation (SE-PSD; AM-PSD) were placed in the pelvic bone. Three implants per group were examined histologically and six implants were tested biomechanically. After 2 and 8 weeks the bone-to-implant contact (BIC) total values of SE implants (43.7 ± 12.2; 53.3 ± 9.0 %) and SE-PSD (46.7 ± 4.5; 61.7 ± 4.9 %) as well as AM implants (20.49 ± 5.1; 43.9 ± 9.7 %) and AM-PSD implants (19.7 ± 3.5; 48.3 ± 15.6 %) showed no statistically significant differences. For SE-PSD and AM-PSD a separate analysis of only the cancellous BIC demonstrated a statistically significant difference after 2 and 8 weeks. Biomechanical findings proved the overall increased stability of the porous implants after 8 weeks. Overall, the great effect of implant macro design on osseointegration was further supported by additional phosphoserine-tethered dendrons for SE and AM implants.

1 Introduction

In orthopedic as well as in oral and maxillofacial surgery there is an increasing demand for reliable primary stability, faster osseointegration and consequently a better implant stability; thus allowing both early loading and good long-term clinical outcome [1, 2]. The manufacturing of implants for fracture fixation and reconstructive surgery mainly relies on the excellent mechanical properties of titanium and its alloys, while bone integration is pursued through innovation in surface treatments where topography is engineered at the nano-, micro- and macro-scale level [3, 4]. Indeed, in the case of dental implant design, the design of thread patterns and pitch distances leads to macro-features which are associated with the improvement of the implant mechanical properties. On the other hand, surface nano-structuring and bio-functionalisation are approaches aiming to enhance biological response mainly through the bio-mimicking of tissue topography and through bioactive material presentation [5]. It has been shown that *ad hoc* surface coatings as well as the combination of hydrophilicity and nanostructures can induce a favourable biological response to the implant [6, 7].

While long-term studies have reported an improved stability of implants engineered with surface treatments,

S. Stübinger · K. Nuss · I. Mosch · M. le Sidler ·
B. von Rechenberg
Musculoskeletal Research Unit, Equine Hospital, Vetsuisse Faculty ZH, University of Zurich, Winterthurerstrasse 260, 8057 Zurich, Switzerland

S. Stübinger (✉) · B. von Rechenberg
Center for Applied Biotechnology and Molecular Medicine (CABMM), Vetsuisse Faculty, University of Zurich, Winterthurerstrasse 190, 8057 Zurich, Switzerland
e-mail: stefan.stubinger@gmail.com; stefan.stuebinger@cabmm.uzh.ch

A. Bürki
Institute for Surgical Biotechnology and Biomechanics, University of Bern, Stauffacherstrasse 78, 3014 Bern, Switzerland

S. T. Meikle · M. Santin
Brighton Studies in Tissue-mimicry and Aided Regeneration, Brighton Centre for Regenerative Medicine, University of Brighton, Huxley Building Lewes Road, Brighton BN2 4GJ, UK

implant failures caused by impaired bone formation during the early stages of implantation can still occur [8], It is widely recognised that a fast biomineralization of the implant surface during the early phase of implantation can favour osseointegration [9].

Phosphoserine is an amino acid known to be the most potent catalyst of biomineralization in the animal kingdom. The molecule is present in the molecular structure of several structural proteins of the extracellular matrix as well as in phospholipids and it has been shown to induce the formation of calcium phosphate crystal formation, hence promoting biomineralization. Past studies have shown the potential of phosphatidylserine coatings to enhance the osseointegration of titanium implants [10]. However, these coatings were relatively thick and of limited stability. In an attempt to simulate the surface nanotopography and biomineralization potential of the phosphatidylserine coatings through a more stable film of synthetic molecules, a new class of hyperbranched peptides was recently developed that was shown to induce fast biomineralization in simulated body fluids as well as to stimulate adult mesenchymal stem cells and osteoblast differentiation [11, 12]. This class of hyperbranched peptides is based on poly (epsilon-lysine) tree-like macromolecules (dendrons) with three branching generations. The uppermost branching generation exposed sixteen units of phosphoserine per molecule and the use of these dendrons as functionalisation molecules for titanium implants also confers a nano-structured topography to their surface. It is believed that the unique ability of this type of monolayer to stimulate biomineralization and osteoblast differentiation is due to the combination of a high density of phosphoserine molecules and the film nanotopography [11].

The present study analyses for the first time the in vivo osseointegrative potential of the phosphoserine-tethered dendron coating applied to dental titanium implants. The research hypothesis was that the use of dendrimeric coating would enhance bone remodelling of two different types of dental implants differing in their designs. By using two different implant types a possible influence of the macro design should be excluded. The stated null hypothesis was that biologically as well biomechanically there would be no significant differences in the osseointegration respectively the bone-to-implant-contact between the two implants independently of the coating application.

2 Materials and methods

2.1 Implants and coating

Titanium alloy (Ti6Al4V) fixtures (diameter 4.1 mm, length 9 mm) underwent the following surface treatments:

(i) a sandblasting and etching (SE); (ii) a macro-porous additive manufacturing (AM) achieved by Direct Metal Laser Sintering (DMLS) (Figs. 1, 2). The implants were fabricated by Eurocoating Spa, Trento, Italy. In this study the AM implants had a cylindrical solid core, 2 mm in diameter, surrounded by a macroporous shell 500 μm in thickness and with a surface porosity of approximately 50 %. A solid thread limited the exposed porosity. The interthreads length was 1.5 mm with a thickness of 500 μm. Porosity was designed according to the gyroid geometry thus having a geometrically ordered and repeated spatial cell unit consisting in a knot with three arms departing with 120° of angular distance. Pores obtained were approximately 500 μm in diameter. After thermal treatment the implants were grinded by manual abrasion with grit paper at one extremity to obtain the hexagon at mechanical tolerances requested for coupling with surgical tools used for insertion and lab tools used for torque out tests. After this step the surface of the part below the hexagon was sandblasted using a resorbable media-blasting agent (i.e. calcium phosphate powder). After this the implants were treated in a phosphoric acid (H_3PO_4) bath to make sure to remove from the surface any eventual blasting agent particles residual. After this step the implants were rinsed in flowing demineralized water with ultra sounds (US) to remove eventual acid residuals. The parts were finally dried in an oven at 60 °C and packaged in a transparent jar presenting a retention tool avoiding the contact of the implant surface with the packaging materials. Packaging in this specialized containers was followed by gamma ray sterilization (Fig. 1).

Machined implants were obtained by a CNC turning machine starting from a bar of Ti6Al4V. The material was chemically the same as the one previously described in the AM series, but the microstructure was different as in this case its morphology was globular. The implants were decontaminated from any residuals contaminant of oil-emulsion by a standard water/detergent solution bath. After this step implants were rinsed in flowing demineralized water under US to remove eventual residuals of detergent from the surface; hence they were passivated in nitric acid and rinsed again. Blasting method used for AM implants was applied (Fig. 2). Scanning electron microscopy (SEM) was performed at 10 keV and at different magnification to provide details of the micro- and nano-scale topography of the implants.

Phosphoserine modified dendron coating was prepared as described by Meikle et al. [13]. Altogether four different groups were analysed: Sandblasted and etched implants (SE), porous additive manufactured implants (AM), SE with additional dendron functionalisation (SE-PSD) and AM with additional dendron functionalisation (AM-PSD).
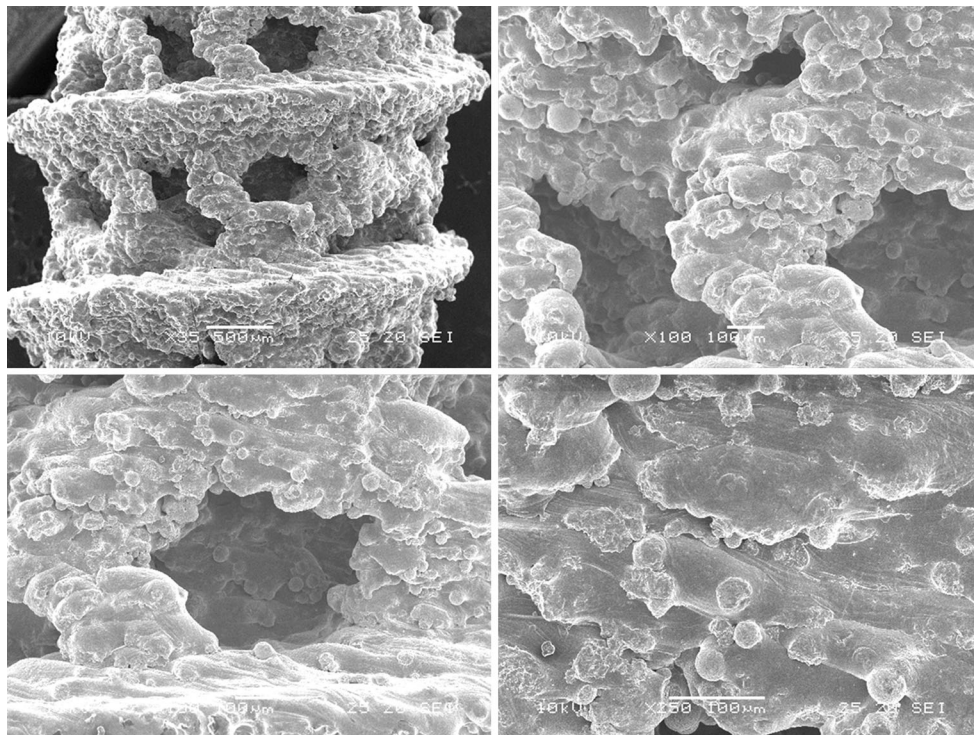
Fig. 1 Scanning electron microscopic images (different magnifications) of the macro-porous additive manufactured implants (AM) achieved by Direct Metal Laser Sintering (DMLS)
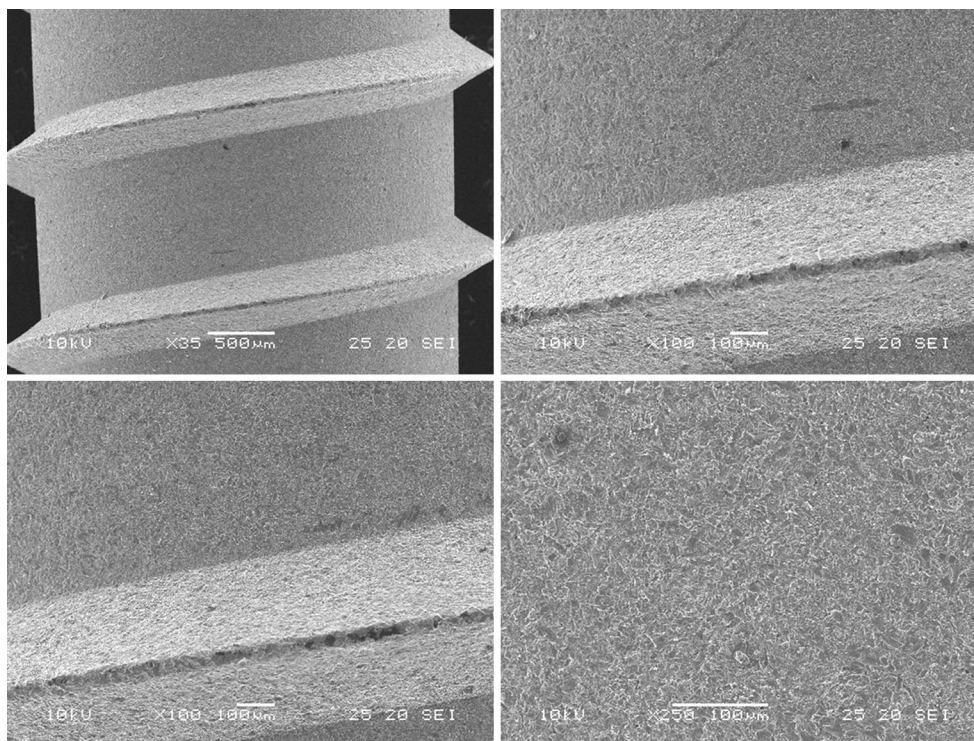

Fig. 2 Scanning electron microscopic images (different magnifications) of implants after sandblasting and etching (SE)

2.2 Experimental animals and surgical model

Six adult, female Swiss Alpine Sheep were used for this study (average age: 3.4 years; average weight: 79.2; 65–90 kg). All experiments were conducted according to the Swiss laws of animal protection and welfare and were authorized by the local federal authorities (authorization #58/2010).

For the experiments a reliable and approved pelvic model in sheep for initial implant screening tests was used [14, 15]. Dental implants were placed in the cranial part of the left and right ileal wing of n = 6 sheep (Fig. 3). On each wing n = 9 implant positions were available which allowed n = 18 implants per animal and a total of n = 108 implants for all animals. However, only n = 72 implants were analyzed in this study. The remaining n = 36 positions were not included in the analysis of the present screening study due to different material characteristics of selected implants in these positions.

For each surface group (SE, SE-PSD, AM, AM-PSD) n = 3 implants were examined histologically (BIC: bone-to-implant-contact) and n = 6 implants were tested with a removal torque-out test. Thus each n = 9 implants were tested per group and time point. Each n = 3 sheep were euthanized after 2 and 8 weeks. By this approach each individual animal had n = 2 implants of each surface group for the biomechanical analysis and n = 1 implant for the histological analysis.

2.3 Anaesthesia

Sheep were sedated with xylazine (0.1 mg/kg BW Rompun® 2 %, Bayer Health Care, Provet AG Lyssach, Switzerland) and buprenorphine (0.01 mg/kg BW Temgesic®, Essex Chemie AG, Luzern, Switzerland). Anaesthesia was induced with diazepam (0.1 mg/kg BW Valium®, Roche
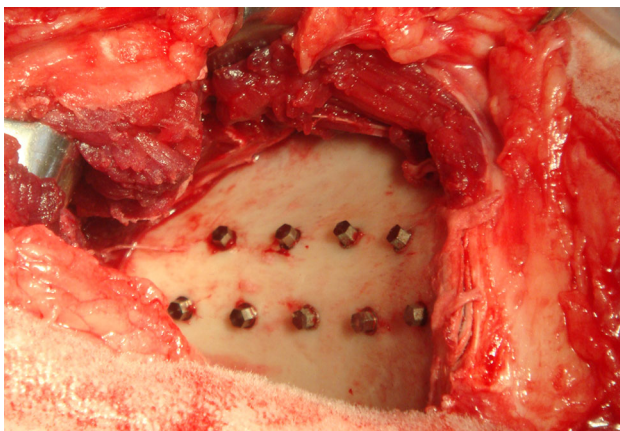

Fig. 3 Intraoperative overview of the *right* pelvis with *nine* implants in situ

Pharma AG, Reinach, Switzerland), ketamine (3–5 mg/kg BW Narketan 10®, Vetoquinol AG, Belp-Bern, Switzerland) and propofol (0.2 mg/kg BW 1 % MCT Fresenius®, Fresenius Kabi AG, Stans, Switzerland). Anesthesia was maintained with inhalation anesthesia (1–1.5 % isoflurane (Forene®, Abbott AG, Baar; Switzerland)) under constant intravenous fluid application (Lactate Ringer 10 ml/kg BW/h) and propofol-infusion (1 mg/kg BW/h) using an injection pump and monitoring (pulse oxymetry, capnography, EKG, invasive blood pressure monitoring). Analgesia was achieved with an additional epidural anesthesia (morphine-HCl 0.1 mg/10 kg BW, Sintetica SA, Mendrisio, Switzerland) at the foramen lumbosacrale during surgery and injection of carprofen (4 mg/kg BW Rimadyl®, Pfizer AG, Zurich, Switzerland) for 4 days. Buprenorphine (0.01 mg/kg BW Temgesic®, Essex Chemie AG, Luzern, Switzerland) was given perioperatively and continued 3 times at 4 h intervals. Tetanus serum (3000 IE Intervet®, Veterinaria AG, Zurich, Switzerland) and antibiotics (Penicillin Natrium Streuli®, Streuli Pharma AG Uznach, Switzerland 30,000 IE/kg BW and Gentamycin—Vetagent®, Veterinaria AG, Zurich 4 mg/kg BW) were given prophylactically.

2.4 Surgical procedure and postoperative care

Sheep were placed in lateral recumbency. Access to the pelvis was achieved by a 15–20 cm long slightly curved skin incision in the longitudinal direction of the iliac bone at the mid-pelvis line. The fascia was cut and the middle gluteal muscle and tensor fasciae lata was carefully separated. The tendinous insertion of the deep and middle gluteal muscles was separated close to the iliac wing in the lower third of the muscle insertions at the iliac crest.

Implant sites were prepared according to a standard drilling protocol using rotating pilot and twist drills in ascending order (diameter). During surgery, a prefabricated flexible and removable template visualized the implantation scheme. Four screws were inserted dorsally and five distally to the linea glutea. All implant drill holes displayed the outer diameter of the implant screws (4.1 mm). Thereby an ideal fit without any press-fit effect or peri-implant bone condensation was possible (Fig. 3). Implant drill holes were about 0.5 mm deeper than the final implant length. After manual implant placement, muscles and soft tissues were repositioned and fixed with synthetic resorbable sutures (Polyglactin; Vicryl 2-0; Johnson&Johnson Int., Brussels, Belgium). Gauze was applied as a protection for the wound before the animal was turned over to the other side. The surgical procedure was repeated in an identical manner on the contralateral pelvis. Postoperatively sheep were kept in small boxes for 2 weeks and then transferred to larger stalls for the remainder time of the

study. After 2 and 8 weeks, the sheep were sacrificed. Implant placement was performed by an experienced surgeon in oral surgery.

2.5 Intravital fluorescence markers

Fluorescence dyes were used to follow dynamic calcium deposition over time. After intravenous or subcutaneous application, these fluorescent probes bind to calcium in the blood stream and are incorporated as hydroxyapatite crystals in newly deposited and mineralized bone matrix (12–72 h after application). Fluorescence dyes were applied at 11, 28 and 53 days. Fluorescence labelling was performed with calcein green (1 ml/kg; Fluka AG, Buchs, Switzerland), xylenolorange (1 ml/kg; Fluka AG, Buchs, Switzerland) and oxytetracyclin (20 mg/kg KGW s.c.; Engemycin® 10 %, Intervet ad us. Vet., Veterinaria AG, Freienbach, Schweiz). These fluorescent dyes were detected in histology sections with a fluorescence microscope (LeicaDM6000B, Camera DFC350 FX Leica Microsystems, Glattbrugg, Switzerland) equipped with the appropriate filters (L5 for calcein green, N3 for xylenol orange, D for oxytetracyclin) giving an indication at the time at which new matrix was deposited over time. This data help to support findings of histomorphometry concerning new bone formation.

2.6 Harvesting of the specimens

The pelvis was harvested immediately after slaughtering and screws were identified through scraping off partially overgrown periosteal bone from the screw heads. Screws were checked for a stable fit and loosening. Radiographs (two views, 55 kV/12 s, 60 kV/12 s) of each half pelvis were made using a Faxitron machine (LX 60 Laboratory Radiography System®, faxitron x-ray corporation, Lincolnshire, IL). Implants and adjacent bone (at least 1 cm) were separated into small blocks using a band saw (KOLBE Nirotechnik Maschinenbau, Riniker AG, Rupperswil, Switzerland). Specimens for removal torque tests were wrapped in moist gauzes, sealed in plastic bags, and kept cool (4 °C) for 24 h until tests were performed.

2.7 Histological preparation

Specimens were fixed in 40 % ethanol at 4 °C and further dehydrated in an ascending series of ethanol (50, 70, 80, 90, 96, 100 %). Afterwards they were defatted in xylene under vacuum. Probes were cut parallel to the implant axis such that serial cuts could be performed after embedding and an exact splitting of the implants along the long axis was achieved. Then probes were infiltrated with methylmethacrylate (Methacrylacidmethylester—Fluka Chemie

GmbH, Buchs, Switzerland; Dibutylphthalat—Merck-Schuchardt OHG, Hohenbrunn, Germany; Perkadox 16—Dr. Grogg Chemie AG, Stetten, Switzerland). Von Rechenberg et al. provide a detailed description of the technique [16]. Ground sections were surface stained with toluidine blue.

A semi-quantitative evaluation of the bone to implant contact (BIC), peri-implant bone remodeling and the presence of a fibrous capsule were made using the stained ground sections. The semi-quantitative analysis allowed assigning approximate measurements rather than an exact measurement that was not feasible in the present case. The percentage of BIC was estimated from calibrated digital pictures since the irregular surface of the implants made quantitative measurements impossible. As such, each side of the implant was subdivided into four equal sectors per side. The coronal cortical and apical parts were measured separately. Thus altogether six sectors were available for the analysis. This approach allowed a separate analysis of cortical and cancellous bone structures adjacent to the implants.

2.8 Histomorphometry

Sections were digitally recorded with a macroscope (Leica M420, Camera DFC 320, Leica Microsystems, Heerbrugg, Switzerland; magnification 0.5 × 8) using a specialized software (Leica, IM 1000 Image manager). Both sides of the implants were digitized, visualizing the bone-implant interface at the threads. Using Adobe Photoshop Elements 8 (Adobe Photoshop 3.0) (Adobe Systems, Inc. San Jose, California, United States), zones around the implants were framed such that the area of new bone or fibrous tissue formation could be measured close to the implant and within threads as well as adjoining the implant. The various tissues were detected manually using the Adobe Photoshop program giving each fraction a different color (new bone, old bone matrix, granulation/fibrous tissue). Old and new bone matrix could be distinguished according to color (light blue = old matrix, dark blue = new matrix). These fractions were then measured with a special analysis software software (QIPS/QWIN, Leica standard, V.3.0, 2003, Leica-Microsystems, Heerbrugg, Switzerland) and a standardized macro-routine using binary segmentation and the different fractions were automatically detected and the pixels measured. In each specimen two predefined and standardized areas on each implant side were evaluated separately. The first area was denominated "Interface" and covered the area within the threads, while the second area was covering the area immediately outside of the threads and was denominated "Surrounding". Results were exported into a spreadsheet (Excel, Microsoft Office 2010) where the percentage of each fraction/total tissue volume and zone was calculated.

2.9 Removal torque test

Tests were performed according to the technique described by Plecko et al. [17]. Briefly, bone blocks were mechanically fixed in dental plaster (Dental Plaster.

GC FujirockVR EP, GC Europe, Leuven, Belgium) and implant heads were connected to the actuator of a servo-hydraulic test machine (MTS Mini Bionix 858, MTS Systems Corporation, Eden Prairie, USA). Rotating the actuator counter-clockwise at 0.1° per second started removal torque testing. The torque removal values (Nmm) were determined with a custom algorithm (Matlab, The MathWorks Inc.).

2.10 Statistical evaluation

Statistical analysis was carried out with SPSS (SPSS Statistics 19, Mac OS X, Version 13.0, Chicago, Illinois, United States). A factorial analysis of variance (ANOVA) was used to test for statistically significant differences, with Bonferroni post hoc tests for inter-group comparisons. Significance was set at $P < 0.05$.

3 Results

3.1 Surgery and postoperative period

Figures 1 and 2 clearly show the different surface morphology of the two types of treatments prior to deposition of the dendrimeric coating. The SEM images clearly show that the topography of the AM implants has a higher porosity than that of the SE devices. The thin layer of dendrimers previously shown by Meikle et al. [13] as a nanotexture morphology could not be discriminated on these surfaces (data not shown). Surgery and anaesthesia were uneventful. Only one sheep displayed a minor wound dehiscence, because of a loosened suture. Suture could be readapted and all sheep showed normal food and water intake 2 days after surgery. No implant exhibited clinical instability. Ventro-dorsal and latero-lateral radiographs demonstrated that all implants were correctly in place and there were no signs of inflammation, osteolysis or fracture lines. Microradiographic images were in accordance with the histological images and thus were not additionally analyzed (Figs. 4, 5).

3.2 Histological evaluation and BIC

After 2 weeks BIC total values of SE implants (43.7 ± 12.2 %) and SE-PSD (46.7 ± 4.5 %) revealed no statistical significant differences to each other (Table 1). Histological examination showed evidence of new bone formation around the surface of uncoated SE implants where
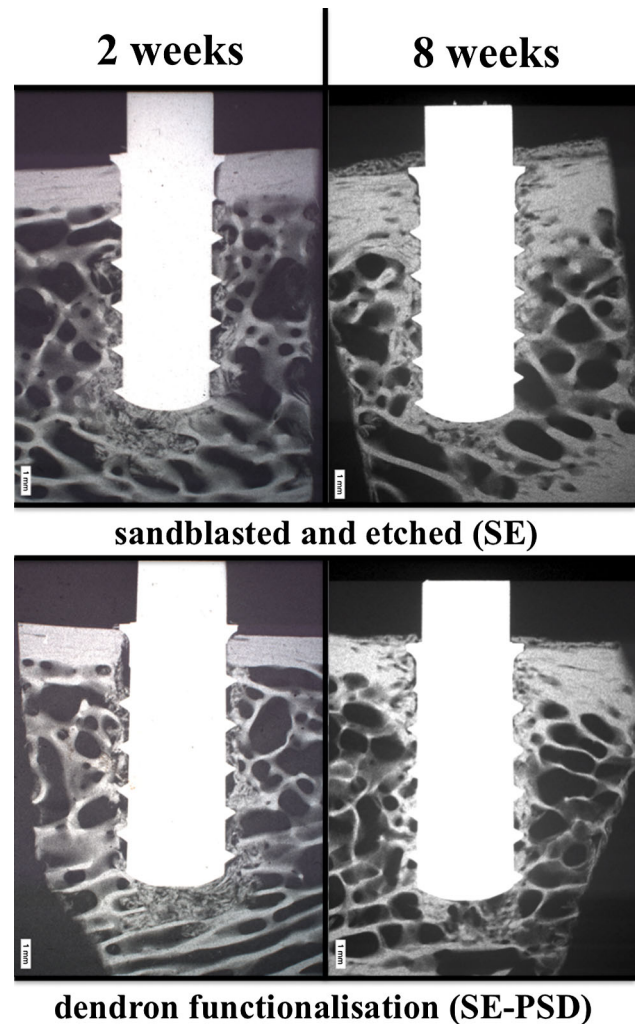

2 weeks | **8 weeks**

sandblasted and etched (SE)

dendron functionalisation (SE-PSD)

Fig. 4 Microradiographic images of SE and SE-PSD implants after 2 and 8 weeks. After 2 weeks bone particles are clearly visible at the apical part at both implants. After 8 weeks a detailed radiodense zone around both implant types is obvious

trabeculae started to surround the implant thread contours. New bone matrix mainly originated from bone chips interposed between the implant and bony walls. The native cortical bone was still in close contact with the implant surface. There were no signs of massive resorption or crater-like bone loss. Peri-implant bone formation of SE-PSD implants demonstrated randomly oriented and very dense trabecular bone meshes. Bone anchors from the surrounding bone debris as well as cancellous bone structures already started bridging the gaps between primary drill channels and implant surfaces (Fig. 6). Likewise, AM implants (20.49 ± 5.1 %) disclosed no statistical significant differences in BIC values when compared to AM-PSD implants (19.7 ± 3.5 %). The histological images showed that, although the overall AM implants BIC values were lower, the trabecular bone disclosed areas of high activity characterised by domains of tight, dark-blue meshes (new bone) of
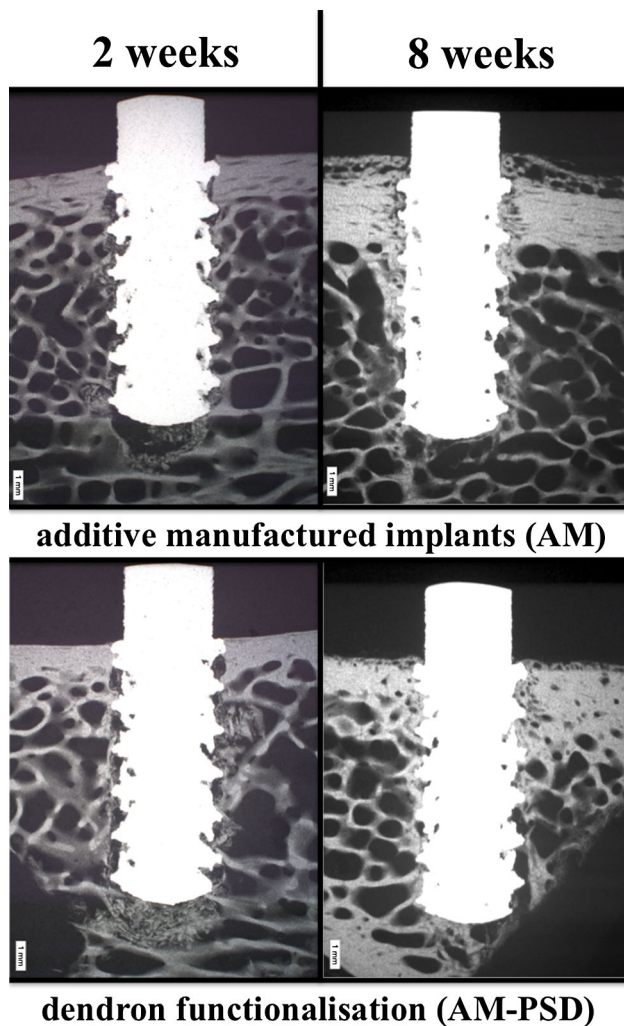
2 weeks | 8 weeks

additive manufactured implants (AM)

dendron functionalisation (AM-PSD)

Fig. 5 Microradiographic images of AM and Am-PSD implants after 2 and 8 weeks. After 2 weeks both implant types reveal a close contact tot he adjacent bone with bony remnants at the apex. After 8 weeks both implants are surrounded by a continuous layer of a radiodense bone matrix

relatively small trabeculae. This process was more evident in proximity of the surfaces coated with phosphoserine-tethered poly(epsilon-lysine) coatings. Yet, BIC was notably heterogenous with some areas showing higher and other showing lower values of BIC (Fig. 7).

After 8 weeks although no statistical significant differences in BIC values was observed between SE (53.3 ± 9.0 %) and SE-PSD (61.7 ± 4.9 %) implants as well as AM (43.9 ± 9.7 %) and AM-PSD (48.3 ± 15.6 %) implants, slightly higher values were observed for the dendron-coated implants. Overall, only for AM-PSD implants the increase of BIC from 2 to 8 weeks was statistical significant ($P = 0.01$). Peri-implant cortical and cancellous compartments demonstrated a high degree of remodeling. Randomly oriented woven bone structures extended from the old parent lamellar bone into the macro-threads of the implants. The

margins of the original drill holes were not visible anymore. Especially at SE-PSD implants an intensive dark-blue zone of new matrix was covering the complete implant. This area extended from the implant's interface into the surrounding tissue and was thus not limited to the contact zone between implant surface and osteotomy walls. Bone debris was almost completely remodelled. AM implant histology showed a comparable bone formation between non-coated AM and AM implants coated with dendrons. Bone debris was entrapped between implant threads and osteoid bands as well as newly formed bone. All implants were embedded into a solid structure of new bone formation.

In a separate analysis of only the cortical BIC no statistically significant differences between all groups and time points could be found. In contrast a separate analysis of only the cancellous BIC demonstrated a statistically significant ($P = 0.01$) difference between SE (46.5 ± 8.2 %) and AM (16.5 ± 1.1 %) implants after 2 weeks. For SE-PSD (2 weeks: 47.2 ± 2.2 %; 8 weeks: 73.1 ± 7.8 %) and AM-PSD (2 weeks: 14.7 ± 1.6 %; 8 weeks: 43.7 ± 8.9 %) a statistically significant difference after 2 and 8 weeks ($P < 0.001$) was obvious.

Furthermore, SE-PSD ($P < 0.001$), AM ($P = 0.05$) and AM-PSD ($P = 0.01$) implants showed statistically significant increase of cancellous BIC values from 2 to 8 weeks.

3.3 Histomorphometric evaluation

Histomorphometrically, in all groups a subsequent percentage gain of new matrix values from 2 to 8 weeks could be detected in the spongiosa (Table 2). AM-PSD revealed the highest increase (2 weeks: 10.5 ± 7.5 %; 8 weeks: 15.7 ± 14.1 %). Correspondingly, after 8 weeks all groups disclosed an increased amount of mature matrix and decreased amount of fibrous tissue in comparison to 2 weeks. For SE implants the decrease of fibrous tissue was statistically significant ($P < 0.001$). An additional evaluation of new bone formation in the interface as well as in the surrounding regions demonstrated that new matrix formation was statistically significant higher in the interface at all groups at 2 and 8 weeks, except for AM at 2 weeks ($P = 0.08$). Yet there was no statistical significant difference between corresponding uncoated and dendron-coated implants. Overall, the amount of mature matrix increased and the amount of fibrous tissue decreased in the interface as well as in the surroundings from 2 to 8 weeks. The only statistically significant difference ($P = 0.02$) could be detected for matrix of AM-PSD implants after 2 weeks.

3.4 Fluorescence labeling

After 2 weeks, obvious signs of a high metabolic activity were observed mainly very close to the implant's surface.

Table 1 Total, cortical and cancellous bone-to-implant-contact (BIC) in % after 2 and 8 weeks

Implant type	BIC total		BIC cortical		BIC cancellous	
	Mean	Standard deviation	Mean	Standard deviation	Mean	Standard deviation
SE—2w	43.7	12.2	42.3	23.8	46.5	8.2
SE—8w	53.3	9.0	33.7	10.8	62.2	15.1
SE-PSD—2w	46.7	4.5	55.2	22.2	47.2	2.2
SE-PSD—8w	61.7	4.9	40.0	15.7	73.1	7.8
AM—2w	20.5	5.2	38.3	26.2	16.5	1.1
AM—8w	43.9	9.7	65.7	23.2	40.5	6.9
AM-PSD—2w	19.7	3.5	37.7	16.4	14.7	1.6
AM-PSD—8w	48.6	9.3	63.2	18.2	43.7	8.9

No significant changes could be observed between the experimental groups

SE sandblasted and etched, *SE-PSD* sandblasted and etched/coated, *AM* additive manufactured, *AM-PSD* additive manufactured/coated

Residual bone particles at the apex of the implant seemed to undergo more intense remodelling than other areas of the implant. Considerably, remodelling processes were happening in cancellous bone. Cortical bone remodeling seemed to be negligible at that stage of healing.

Fluorochrome labeling at 8 weeks disclosed only small areas of bone remodelling. Active processes that could be demonstrated with polychrome labeling seemed to have ceased at that time. Fluorescence labelling clearly showed evidence of continuous bone maturation in form of trabeculae and lacunae (Fig. 8). Overall, however, no striking differences could be detected (Fig. 9).

3.5 Evaluation of removal torque test

SE implants showed no statistical significant increased torque values after 2 weeks (677.9 ± 89.4 Nmm) and 8 weeks (730.1 ± 151.9 Nmm) in comparison to SE-PSD implants (2 weeks: 587.4 ± 111.6 Nmm; 8 weeks: 812.2 ± 147.9 Nmm). There was also no statistical significant difference between AM implants (2 weeks: 785.0 ± 146.7; 8 weeks: 1,891.8 ± 308.4 Nmm) and AM-PSD implants (721.3 ± 185.5 Nmm; 1,754.96 ± 613.4 Nmm) at corresponding time points (Table 3).

However, there was statistical significant difference after 8 weeks between SE and AM ($P = 0.00$) implants as well as SE-PSD and AM-PSD ($P = 0.00$) implants. Additionally, AM and AM-PSD implants demonstrated a statistical significant increase of torque values from 2 to 8 weeks ($P = 0.00$).

4 Discussion

To study osseointegration several animal models are described in the literature [18, 19]. Rabbit models are commonly used owing to their cost effectiveness and associated easy of surgery [20]. However, rabbits have a faster skeletal bone remodelling and the anatomical dimensions of the rabbit tibia and femur allow only the implantation of devices with a mean length of about 8–10 mm [21]. Canine models are another alternative and represent a well-established animal model in modern implantology [22]. However, a 2.5-fold higher bone remodelling rate, mainly cortical bone structures, postoperative complications like poor mouth hygiene and ethical reason excluded this model for the present research question [23].

In contrast the pelvic bone of sheep offers sufficient quantity and quality of cancellous as well as cortical bone structures. This allows for a separate and specific evaluation and analysis of the influence of characteristic implant features. In the present study coating of dental implants with phosphoserine-tethered poly(epsilon-lysine) dendrons of three branching generation showed an ability to stimulate the early formation of trabecular bone at the implant/tissue interface, but no significant advantage over the formation of cortical bone. It can be speculated that the early biomineralization of the surface—when in contact with blood electrolytes—as well as the induced osteoblast adhesion and differentiation triggered by the biomineralized and nano-texturised surface has been responsible for a relatively high bone regeneration activity. This activity is seen by the presence of a tight network of relatively small trabeculae invading the peri-implant space in the case of dendron-coated samples. The avoidance of any press-fit effect with distinct marginal bone condensation and crack formation in the cancellous bone may have further supported this process [24, 25]. Beyond the biological effect promoted by the biomimetic coating, the direct mechanical tissue trauma induced by the drilling and the implant insertion procedure itself may have stimulated a distinct new matrix formation especially directly at the implant-bone-interface [26]. The particular character of the bone healing process at the implant/tissue interface was
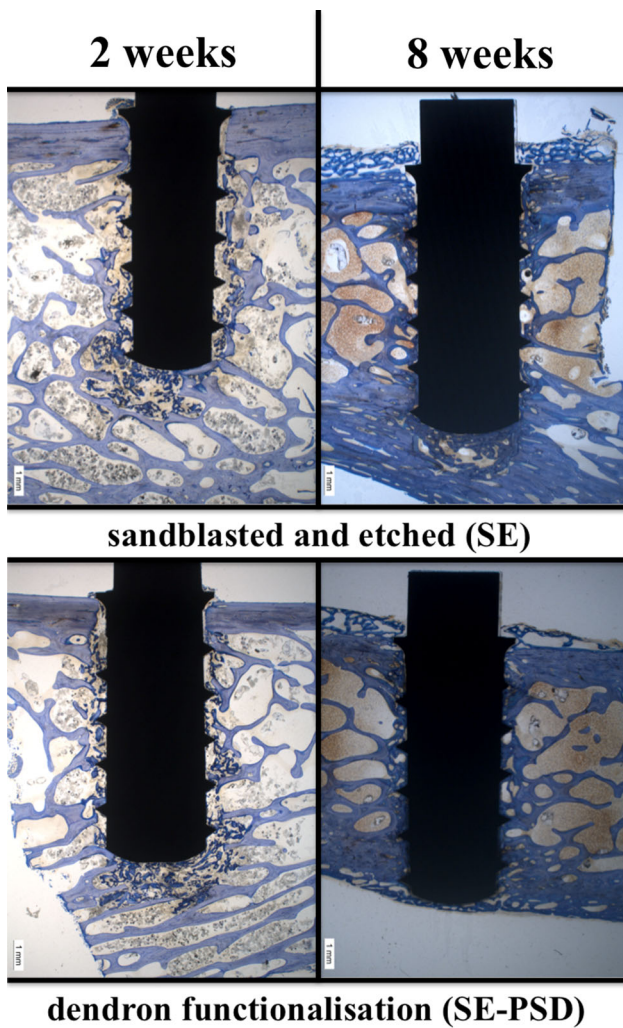
Fig. 6 Toluidine-stained thick sections of SE and SE-PSD implants after 2 (*left*) and 8 (*right*) weeks. After 2 weeks the osteotomy walls are still visible. Bone debris is loosely packed into the trabecular structures of the cancellous compartment. After 8 weeks the initial gaps between implants and osteotomy sites are filled with new bone matrix. Lateral bony anchors have a direct contact to the implant surface. SE-PSD implants are thoroughly encompassed by a highly dense trabecular network

Fig. 7 Toluidine-stained thick sections of AM and AM-PSD implants after 2 (*left*) and 8 (*right*) weeks. After 2 weeks the voids between the threads are partly filled with bone debris. Implants have a close cortical and cancellous bone contact. After 8 weeks cortical bone remodelling leaves a porous zone at the coronal interface. Overall a broad zone of trabecular is visible at both interfaces

emphasised by the physiological and undistributed bone remodelling of reduced turnover rate observed in the areas of mature bone tissue found at relatively longer distance from the implant surface.

The present study also demonstrated that bone repair was determined not only by the thin dendrimeric coating, but also by the underlying macro design of the implant. However, as the highly ragged surface of the AM implant surface made the quantitative BIC measurement relatively challenging, final conclusions cannot be drawn. According to the classical concept of primary bone ingrowth onto a porous surface, AM as well as AM-PSD implants revealed an increased potential for primary stability as new bone formation (i.e. BIC values) significantly increases from 2 to
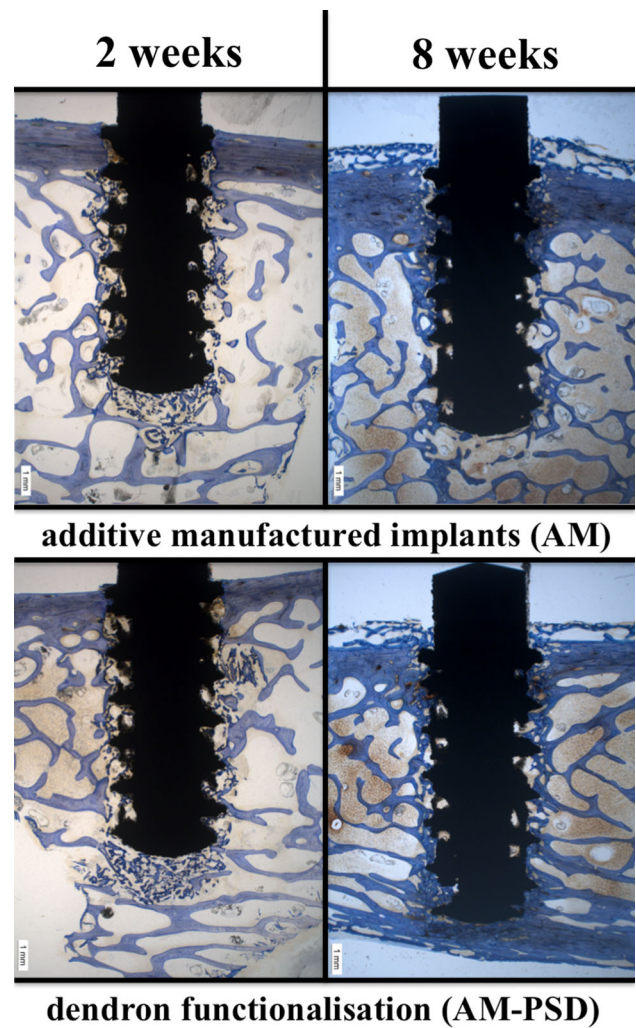
8 weeks [27]. As highlighted above, a more cancellous bone is considered to be more advantageous for this process than a dense, pseudo-cortical bone formation. However, these findings were critically affected by the low measurable initial contact of implants in the cancellous part after 2 weeks. Strikingly, the porous implants attenuated the minor press-fit contact in the cortical compartment, whereby the cortical BIC line increased from 2 to 8 weeks in comparison to SE implants. Hence, it can be assumed that the macroporosity could protect the biomimetic dendron coating from damages during the implantation procedure.

Biomechanical findings proved the overall trend of an increased stability of the porous implants after 8 weeks. However, as the mineralisation of the new matrix after

Table 2 Comparison of new, old and soft tissue matrix formation in (%) at the interface, surrounding, spongisa and cortex

Implant type	New matrix				Old matrix				Fibrous tissue			
	Interface	Surrounding	Spongiosa	Cortex	Interface	Surrounding	Spongiosa	Cortex	Interface	Surrounding	Spongiosa	Cortex
SE—2w	21.4 ± 6.8	7.0 ± 3.7	14.4 ± 8.6	14.0 ± 10.0	31.1 ± 20.5	47.4 ± 27.1	27.6 ± 9.5	50.9 ± 30.2	47.5 ± 23.5	45.7 ± 27.3	58.1 ± 8.9	35.1 ± 30.5
SE—8w	28.4 ± 19.8	7.7 ± 8.3	15.5 ± 19.0	20.6 ± 18.0	45.7 ± 16.5	64.8 ± 15.9	48.6 ± 15.0	61.9 ± 20.1	25.8 ± 9.6	27.5 ± 17.7	35.8 ± 12.4	17.5 ± 8.4
SE-PSD—2w	17.3 ± 9.9	2.8 ± 3.6	9.9 ± 9.9	10.3 ± 11.3	42.6 ± 22.9	58.5 ± 18.7	35.8 ± 10.6	65.2 ± 20.7	40.1 ± 19.2	38.7 ± 19.1	54.3 ± 7.2	24.5 ± 14.2
SE-PSD—8w	16.9 ± 8.3	2.8 ± 3.0	10.1 ± 9.6	9.7 ± 9.5	55.8 ± 10.1	65.6 ± 16.8	52.5 ± 9.4	68.9 ± 14.2	27.2 ± 9.8	31.6 ± 17.6	37.4 ± 13.7	21.4 ± 9.5
AM—2w	14.9 ± 8.7	2.2 ± 2.0	7.6 ± 6.0	9.5 ± 11.6	36.5 ± 15.4	61.3 ± 27.3	32.8 ± 9.5	65.0 ± 25.8	48.6 ± 12.6	36.5 ± 26.2	59.6 ± 6.0	25.6 ± 16.1
AM—8w	17.8 ± 7.7	3.8 ± 3.5	9.0 ± 7.2	12.5 ± 11.0	49.7 ± 11.7	62.1 ± 18.7	46.8 ± 9.2	65.0 ± 17.5	32.5 ± 11.2	34.1 ± 18.2	44.1 ± 11.0	22.5 ± 9.2
AM-PSD—2w	18.5 ± 7.3	3.5 ± 2.1	10.5 ± 7.5	11.5 ± 11.1	26.1 ± 6.3	55.6 ± 17.0	32.6 ± 9.8	49.2 ± 23.6	55.4 ± 8.1	40.9 ± 15.8	57.0 ± 5.5	39.3 ± 15.1
AM-PSD—8w	25.7 ± 16.0	9.4 ± 10.2	15.7 ± 14.1	19.4 ± 17.3	42.8 ± 16.4	55.0 ± 21.9	38.7 ± 14.7	59.1 ± 19.6	31.4 ± 12.0	35.6 ± 18.5	45.6 ± 10.6	21.4 ± 8.1

SE sandblasted and etched, *SE-PSD* sandblasted and etched/coated, *AM* additive manufactured, *AM-PSD* additive manufactured/coated

8 weeks was not completely finished, no significant differences between coated and uncoated implants could be detected. The favourable gain of new bone with an increased BIC line and new matrix formation was probably biomechanically still not stable enough to withstand the high torque values. By selecting a later time point (12 weeks) this effect could have been attenuated. Thus for a comprehensive and critical evaluation of new implant macro-designs and surface modifications a combined biomechanical and biological analysis is essentially important to avoid any misleading conclusion about the potential clinical benefits of the biomimetic dendron coating.

In particular, the interpretation of static histological parameters like such as the BIC should be made with caution, as they often do not accurately reflect the dynamic and notably biomechanical properties of the bone-implant interactions [28, 29]. Likewise recent published studies, the present investigation revealed some striking discrepancies between biomechanical and static histological results [30]. Whereas the BIC for AM implants was generally inferior to SE and SE-PSD implants, biomechanical stability data showed better performances in AM implants after 8 weeks. These differences could be explained only through the help of further dynamic evaluation studies.

Overall, for testing osseointegration and bone remodeling the chosen animal in sheep has turned out to be highly beneficial, because of biological, technical, and statistical advantages. Yet one limiting factor was the overall limited number of animal used. Thus for confirming the present findings additional analyses especially regarding soft tissue performance are necessary.

5 Conclusion

In the present study the use of a phosphoserine-tethered poly(epsilon-lysine) coating revealed its beneficial effect over the rapid formation of new bone, hence osseointegration, of sandblasted and etched surfaces as well as on macro-porous additive manufactured implants especially when implanted in cancellous bone structures. Uniquely, the present study provided a demonstration that the clinical performance of this type of innovative coating also depends on the macro-topography of the underlying surface that may have an impact both on the biological response and on the protection of the organic macromolecular layer deposited on the implant surface. The difference in SE and AM preparation could be made even more prominent by using this coating. With its histological features, the pelvic sheep model allowed a clinically-reflective assessment of the fixture performance in an anatomical site similar to the jaw where both cortical and cancellous bone integration is required.

Fig. 8 Fluorochrome labelling after 2 weeks. A high metabolic activity were observed mainly very close to the implant's surface. Additionally, an intensive area of bone remodelling showed up at the apical part of the implants due to incongruity of implant length and drill hole
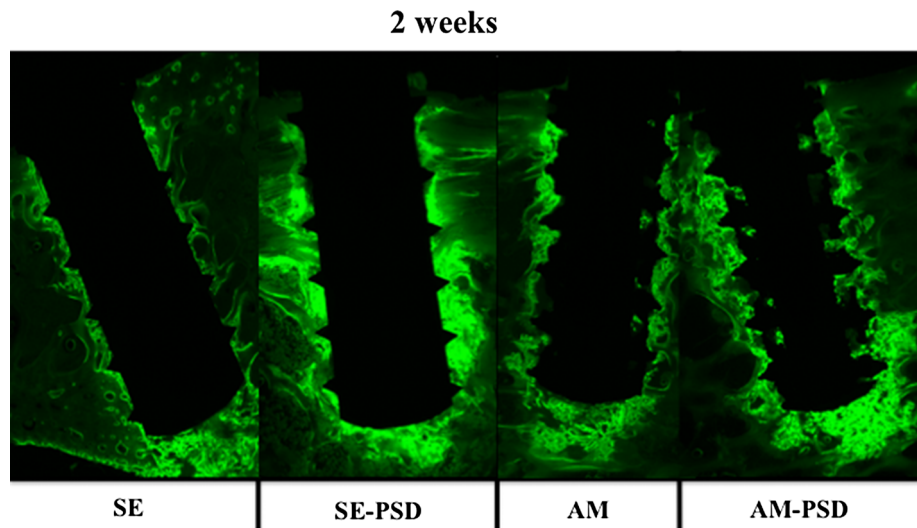

2 weeks

SE | SE-PSD | AM | AM-PSD

Fig. 9 Fluorochrome labelling after 8 weeks. At the cancellous bone compartment a conspicuous zone of active bone remodelling with a clear tendency of lateral expansion is marked by the fluorochromes. Calcein *green* labelling is highly active. Xylenolorange and oxytetracyclin demonstrate an increased remodelling at the cortical layer (Color figure online)
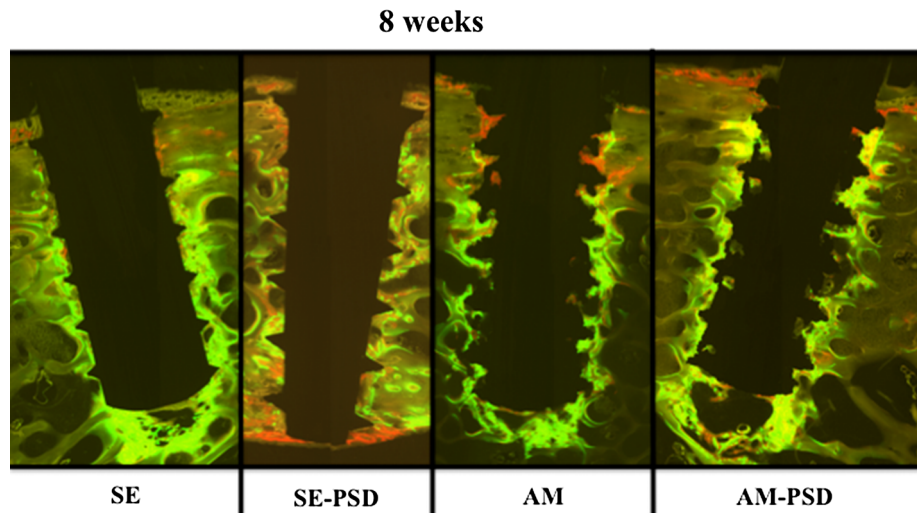

8 weeks

SE | SE-PSD | AM | AM-PSD

Table 3 Comparison of removal torque values in (Nmm) after 2 and 8 weeks

Implant type	Torque values in Nmm	
	Mean	Standard deviation
SE—2w	677.9	89.4
SE—8w	730.1	151.9
SE-PSD—2w	587.4	111.6
SE-PSD—8w	812.2	147.3
AM—2w	785.0	146.7
AM—8w	1,891.8	308.4
AM-PSD—2w	721.3	185.5
AM-PSD—8w	1,755.0	613.4

SE sandblasted and etched, *SE-PSD* sandblasted and etched/coated, *AM* additive manufactured, *AM-PSD* additive manufactured/coated

References

1. Banerjee S, Issa K, Kapadia BH, Pivec R, Khanuja HS, Mont MA. Highly-porous metal option for primary cementless acetabular fixation. What is the evidence? Hip Int. 2013;23:509–21.
2. Götz W, Gedrange T, Bourauel C, Hasan I. Clinical, biomechanical and biological aspects of immediately loaded dental implants: a critical review of the literature. Biomed Tech (Berl). 2010;55:311–5.
3. Le Guéhennec L, Soueidan A, Layrolle P, Amouriq Y. Surface treatments of titanium dental implants for rapid osseointegration. Dent Mater. 2007;23:844–54.

4. Palmquist A, Omar OM, Esposito M, Lausmaa J, Thomsen P. Titanium oral implants: surface characteristics, interface biology and clinical outcome. J R Soc Interface. 2010;5:515–27.

5. Tomisa AP, Launey ME, Lee JS, Mankani MH, Wegst UG, Saiz E. Nanotechnology approaches to improve dental implants. Int J Oral Maxillofac Implants. 2011;26:25–44.

6. Richards RG, Moriarty TF, Miclau T, McClellan RT, Grainger DW. Advances in biomaterials and surface technologies. J Orthop Trauma. 2012;26:703–7.

7. Wennerberg A, Jimbo R, Stübinger S, Obrecht M, Dard M, Berner S. Nanostructures and hydrophilicity influence osseointegration: a biomechanical study in the rabbit tibia. Clin Oral Implants Res. 2013. doi:10.1111/clr.12213.

8. Junker R, Dimakis A, Thoneick M, Jansen JA. Effects of implant surface coatings and composition on bone integration: a systematic review. Clin Oral Implants Res. 2009;20:185–206.

9. Sjöström T, Brydone AS, Meek RM, Dalby MJ, Su B, McNamara LE. Titanium nanofeaturing for enhanced bioactivity of implanted orthopedic and dental devices. Nanomedicine (Lond). 2013;8:89–104.

10. Merolli A, Santin M. Role of phosphatidyl-serine in bone repair and its technological exploitation. Molecules. 2009;14:5367–81.

11. Santin M, Rhys-Williams W, O'Reilly J, Davies MC, Shakesheff K, Love WG, Lloyd AW, Denyer SP. Calcium-binding phospholipids as a coating material for implant osteointegration. J R Soc Interface. 2006;3:277–81.

12. Galli C, Piemontese M, Meikle ST, Santin M, Macaluso GM, Passeri G. Biomimetic coating with phosphoserine-tethered poly (epsilon-lysine) dendrons on titanium surfaces enhances Wnt and osteoblastic differentiation. Clin Oral Implants Res. 2013. doi:10.1111/clr.12075.

13. Meikle ST, Bianchi G, Olivier G, Santin M. Osteoconductive phosphoserine-modified poly({varepsilon}-lysine) dendrons: synthesis, titanium oxide surface functionalization and response of osteoblast-like cell lines. J R Soc Interface. 2013;10:20120765.

14. Langhoff JD, Voelter K, Scharnweber D, Schnabelrauch M, Schlottig F, Hefti T, Kalchofner K, Nuss K, von Rechenberg B. Comparison of chemically and pharmaceutically modified titanium and zirconia implant surfaces in dentistry: a study in sheep. Int J Oral Maxillofac Surg. 2008;37:1125–32.

15. Stübinger S, Biermeier K, Bächi B, Ferguson SJ, Sader R, von Rechenberg B. Comparison of Er:YAG laser, piezoelectric, and drill osteotomy for dental implant site preparation: a biomechanical and histological analysis in sheep. Lasers Surg Med. 2010;42:652–61.

16. von Rechenberg B, Leutenegger CM, Zlinszky K, McIlwraith CW, Akens MK, Auer JA. Upregulation of mRNA of interleukin-1 and 6 in subchondral cystic lesions of four horses. Equine Vet J. 2000;33:143–9.

17. Plecko M, Sievert C, Andermatt D, Frigg R, Kronen P, Klein K, Stübinger S, Nuss K, Bürki A, Ferguson S, Stoeckle U, von Rechenberg B. Osseointegration and biocompatibility of different metal implants—a comparative experimental investigation in sheep. BMC Musculoskelet Disord. 2012;13:32.

18. Auer JA, Goodship A, Arnoczky S, Pearce S, Price J, Claes L, von Rechenberg B, Hofmann-Amtenbrinck M, Schneider E, Müller-Terpitz R, Thiele F, Rippe KP, Grainger DW. Refining animal models in fracture research: seeking consensus in optimising both animal welfare and scientific validity for appropriate biomedical use. BMC Musculoskelet Disord. 2007;8:72.

19. Mills LA, Simpson AH. In vivo models of bone repair. J Bone Joint Surg Br. 2012;94:865–74.

20. Stübinger S, Dard M. The rabbit as experimental model for research in implant dentistry and related tissue regeneration. J Invest Surg. 2013;26:266–82.

21. Pearce AI, Richards RG, Milz S, Schneider E, Pearce SG. Animal models for implant biomaterial research in bone: a review. Eur Cell Mater. 2007;13:1–10.

22. Vignoletti F, Abrahamsson I. Quality of reporting of experimental research in implant dentistry. Critical aspects in design, outcome assessment and model validation. J Clin Periodontol. 2012;39:6–27.

23. Kimmel DB, Jee WS. A quantitative histologic study of bone turnover in young adult beagles. Anat Rec. 1982;203:31–45.

24. Trisi P, Todisco M, Consolo U, Travaglini D. High versus low implant insertion torque: a histologic, histomorphometric, and biomechanical study in the sheep mandible. Int J Oral Maxillofac Implants. 2011;26:837–49.

25. Jimbo R, Tovar N, Yoo DY, Janal MN, Anchieta RB, Coelho PG. The effect of different surgical drilling procedures on full laser-etched microgrooves surface-treated implants: an experimental study in sheep. Clin Oral Implants Res. 2013. doi:10.1111/clr.12216.

26. Tehemar SH. Factors affecting heat generation during implant site preparation: a review of biologic observations and future considerations. Int J Oral Maxillofac Implants. 1999;14:127–36.

27. Deporter D. Dental implant design and optimal treatment outcomes. Int J Periodontics Restorative Dent. 2009;29:625–33.

28. Al-Nawas B, Wagner W, Grötz KA. Insertion torque and resonance frequency analysis of dental implant systems in an animal model with loaded implants. Int J Oral Maxillofac Implants. 2006;21:726–32.

29. Witek L, Marin C, Granato R, Bonfante EA, Campos FE, Gomes JB, Suzuki M, Coelho PG. Surface characterization, biomechanical, and histologic evaluation of alumina and bioactive resorbable blasting textured surfaces in titanium implant healing chambers: an experimental study in dogs. Int J Oral Maxillofac Implants. 2013;28:694–700.

30. Jimbo R, Coelho PG, Bryington M, Baldassarri M, Tovar N, Currie F, Hayashi M, Janal MN, Andersson M, Ono D, Vandeweghe S, Wennerberg A. Nano hydroxyapatite-coated implants improve bone nanomechanical properties. J Dent Res. 2012;91:1172–7.